X-ray crystal structure of cytotoxic oxidized cholesterols: 7-ketocholesterol and 25-hydroxycholesterol

Mary P. McCourt[1,*] Khuram Ashraf,[*] Russ Miller,[†,§] Charles M. Weeks,[†] Naiyin Li,[†] Walter Pangborn,[†] and Douglas L. Dorset[*]

Electron Diffraction Department* and Molecular Biophysics Department,† Hauptman Woodward Medical Research Institute, 73 High Street, Buffalo, NY 14230, and Computer Science Department,§ State University of New York at Buffalo, Buffalo, NY 14260

Abstract The cytotoxic cholesterol derivative, 7-ketocholesterol, crystallizes in a monoclinic unit cell, space group $P2_1$ with a = 11.405 Å, b = 6.288 Å, c = 35.393 Å and β = 92.75° (Z = 4). Its room temperature crystal structure was solved by direct methods, i.e., the minimal principle via the Shake-and-Bake (SnB) algorithm. In contrast to the continuous chain pattern found for the cholesterol monohydrate structure, hydrogen bonding in the 7-ketocholesterol structure is localized to specific sites via one water molecule that forms linkages between two O3 hydroxyl groups and one keto oxygen. The final weighted R factor for 4562 reflections was 0.144. The 25-hydroxycholesterol also crystallizes in a monoclinic unit cell ($P2_1$), with a = 10.840 Å, b = 14.533 Å, c = 16.093 Å and β = 95.91° (Z = 4). The low temperature structure was solved by DIRDIF. In this instance, molecular packing is anti-parallel in layers stabilized by hydrogen bonding networks via both hydroxyl functions, differing both from cholesterol monohydrate and the 7-ketocholesterol. The final weighted R-factor for 6566 reflections was 0.034. Functional differences of the oxysterols therefore, may be expressed by observed variations in the molecular packing and geometry.—**McCourt, M.P., K. Ashraf, R. Miller, C.M. Weeks, N. Li, W. Pangborn, and D.L. Dorset.** X-ray crystal structure of cytotoxic oxidized cholesterols: 7-ketocholesterol and 25-hydroxycholesterol. *J. Lipid Res.* 1997. **38:** 1014–1021.

Supplementary key words oxysterol • atherosclerosis • X-ray crystallography • cholesterol

In recent years there has been considerable interest in the role of lipid oxidation in the cellular events that lead to atherosclerosis (1). Experimental studies with oxysterols have shown that, in general, these compounds are far more atherogenic than cholesterol itself (2) and may in fact be responsible for the primary events leading to the development of the fatty lesion (3). Deposition of cholesterol and its esters in atherosclerotic lesions, on the other hand, is probably not directly responsible for the initiation of the lesion, but is merely a secondary process (4). In addition, Zwijsen, Oudenhoven, and de Haan (5) have shown that oxysterols inhibit intracellular communicating ability of human smooth muscle cells, which may also be a promoting factor in atherogenesis.

Most of the recent attention has been paid to endogenous oxidized lipids (6,7) although evidence for atherogenic behavior of exogenous oxidation products has been recognized since the earliest part of the 20th century. Taylor et al. (2) identified many oxidized cholesterols that are particularly toxic to arterial cells, including 25-hydroxycholesterol, 3β,5α,6β-cholestane triol, and 7-ketocholesterol.

Oxysterols can affect physiological functions in a variety of ways, such as the reduction of cholesterol uptake (8), the inhibition of membrane-bound enzymes (9), and the blockage of carrier-mediated transmembrane hexose transport (9). It was thought that the oxysterol might compete with cholesterol in a lipid bilayer and that the incorporation of the oxidized derivatives in the membranes would drastically alter the surface properties of affected cells, perhaps initiating cell lysis (9). If this is true, studies of their cosolubility with cholesterol may provide some clues about the importance of relative molecular volumes and preferred molecular packing motifs initiated by the presence of additional polar groups on the cholesterol nucleus. That is to say, while the oxidized derivative may freely substitute for the unsubstituted sterol in cell membranes, the accumulation of new molecular interactions may lead to fractionation and hence the cytotoxic effect.

The cosolubility results seen in the phase diagrams of

Abbreviations: 7-ketocholesterol, 5-cholesten-3β-ol-7-one; 25-hydroxycholesterol, 5-cholesten-3β-25-diol.

[1]To whom correspondence should be addressed.

both 25-hydroxycholesterol and 7-ketocholesterol with cholesterol (10) indeed suggest that the molecular volume and shape of these two molecules would allow for their physical substitution for cholesterol in the cell membrane. On the other hand, the marked difference in observed cytotoxicity of 25-hydroxycholesterol and 7-ketocholesterol cannot be explained by such physical measurements as they each have similar phase diagrams with cholesterol. Also, the enhanced toxicity of 3β, 5α, 6β-cholestane triol to arterial cells cannot be explained from the phase diagrams as it is far less soluble in cholesterol than is 7-ketocholesterol (10). Therefore, while the phase diagrams indicate the cosolubility of the oxysterols with cholesterol, these results do not indicate a reason for the differences in their cytotoxicity to arterial cells.

It is possible that such functional differences may be expressed more clearly by comparing the molecular packing and geometry of oxidized cholesterols with that of cholesterol itself. Examination of the differences in the hydrogen bonding of the crystal structures of the oxysterols may also show how these molecules, if substituted for cholesterol in a cell membrane, would disturb normal cholesterol interactions. The crystal structures of 7-ketocholesterol and 25-hydroxycholesterol are reported here as the first in a series of such cytotoxic oxidized cholesterols.

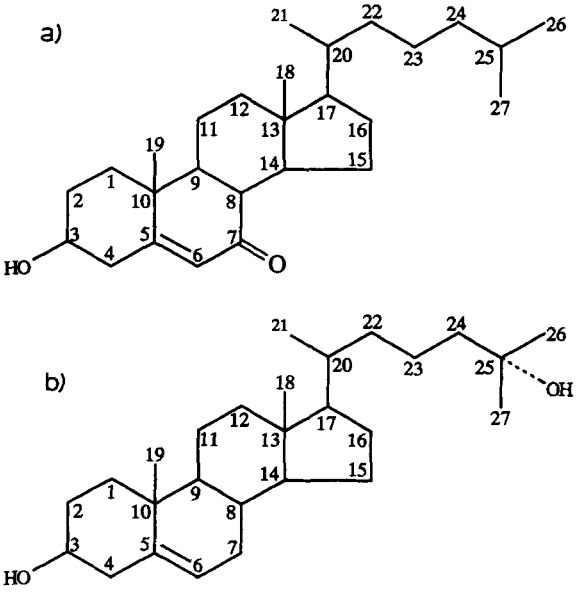

Fig. 1. Numbering scheme for 7-ketocholesterol (a) and 25-hydroxycholesterol (b).

METHODS

Crystal growth

7-Ketocholesterol (5-cholesten-3β-ol-7-one) and 25-hydroxycholesterol (5-cholestene-3β-25-diol) were purchased from Sigma (St. Louis, MO) and were stated to be between 95–97% pure. In both instances, a small unweighed amount was placed in a small glass beaker and then dissolved in methanol. The beaker was covered with Parafilm and the solution was allowed to evaporate at room temperature, eventually producing long, thin lath-like crystals.

X-ray diffraction

7-Ketocholesterol. Unit cell constants and an orientation matrix for data collection were obtained by least squares refinement using the setting angles of 25 centered reflections located on the Enraf-Nonius CAD-4 diffractometer. Intensity data were collected at room temperature using Ni-filtered CuKα radiation, periodically monitoring standard reflections to detect the occurrence of radiation damage to the crystal. In all, 6414 unique reflections were measured, of which 1852 were judged to be unobserved, based on the criterion that $|F_o| < 3.0\ \sigma|F_c|$. The noncentrosymmetric monoclinic space group is $P2_1$ (determined by $k = 2n + 1$ systematic absences in the 0k0 reflections). The cell dimensions are a = 11.405 (3) Å, b = 6.288 (1) Å, c = 35.39 (1) Å, β = 92.75° (1), Z = 4, i.e., with two molecules in the asymmetric unit.

25-Hydroxycholesterol. The crystal was mounted on a glass fiber and all measurements were made on a Siemens/Nicolet diffractometer with CuKα radiation. Cell constants and an orientation matrix for data collection, obtained from a least squares refinement using the setting angles of 50 carefully centered reflections in the range $37.50° < 2\theta < 58.90°$ corresponded to a primitive monoclinic cell with dimensions, a = 10.840 (2) Å, b = 14.533 (2) Å, c = 16.094 (3) Å and β = 95.91° (2) (Z = 4). The data were collected at a temperature of 120 ± 1° K using the ω–2θ scan technique to a maximum 2θ value of 114.4°. Based upon the systematic absences of [0k0]: k = 2n + 1, packing considerations, a statistical analysis of intensity distribution, and the successful solution and refinement of the structure, the space group was determined to be $P2_1$. The scan profile data were corrected for background subtraction, Lorentz and polarization effects. The time-dependent scaling factor, determined from fits to various standard reflections measured after every 200 reflections, was less than 1%. No absorption correction was applied. Of the 17950 reflections that were collected, 6840 were unique. The agreement index for averaging replicate and/or space group equivalent reflections was $R_{sym} = \Sigma\ |F_i^2 - F^2|/\Sigma\ |F_i^2| = 0.018$.

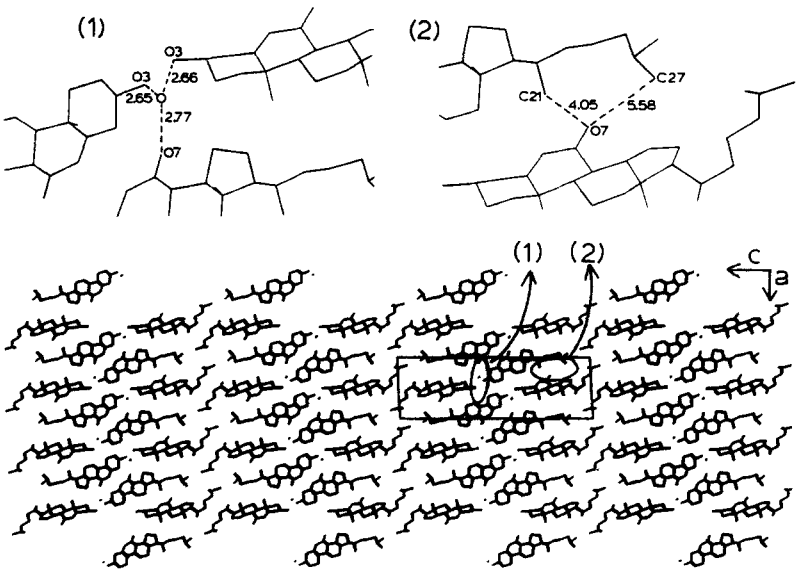

Fig. 2. Packing diagram for 7-ketocholesterol indicating the unit cell in the enclosed box, showing both the hydrogen bonding of the two O3 atoms and the O7 atom of three 7-ketocholesterol molecules with the solvent oxygen (1) as well as the hydrophobic pocket which includes the O7 atom of one of the 7-ketocholesterol molecules (2).

Structure analysis

7-Ketocholesterol. After the observed intensity data were processed using the programs of Blessing (11), the crystal structure (see **Fig 1a** for numbering scheme) was solved by direct methods via a multisolution technique, the Shake and Bake (SnB) algorithm (12). Identification of likely solutions is based on the theory that a particularly simple function of the phases, known as the minimal function (13), has a constrained global minimum at the correct set of phases. After the initial trial phase solutions were processed by a phase annealing step, the map representing the lowest trial minimal function value was examined. Peak positions picked from this initial electron density map corresponded to distinct molecular fragments, i.e., the two cholesteryl nuclei in the asymmetric unit. Atoms in three of the four rings of the cholesterol skeleton were then identified for each of the two molecules, but the isoprenoid side chains were not found.

Using the fractional atomic coordinates from the direct phasing model to calculate trial phased structure factors, a new electron density map was generated, from which additional peak positions were determined. With each iteration of Fourier refinement, new peaks were added to the model until all the atoms in the structure were identified. A final difference Fourier map revealed an additional peak that appeared to be a solitary solvent oxygen model. Subsequent difference maps did not reveal any additional peaks to indicate that it was methanol. Because the methanol used for crystallization was not anhydrous, we feel that the solvent molecule is most likely water as such hydration sites have been found in numerous previous crystal structure analyses (C.M. Weeks, unpublished summary) on steroids grown from non-anhydrous polar solvents (e.g., methanol, ethanol, acetone, ethyl acetate). Furthermore, there is no room in the identified solvation pocket to permit the inclusion of a molecule larger than water. After positions had been completely determined, all the atoms, except those isoprene positions with B values greater than 8.0 $Å^2$, were refined anisotropically by least squares. Due to the high thermal motion in this region, the isoprenoid ends of both molecules were constrained to reflect standard bonding geometries. However, the conformational orientation of the chains found in the structure determination was retained. The final R value, not including hydrogens, was 14.4% and this was not changed when calculated hydrogens were included. High thermal motion may account for this failure to improve the fit to the observed data. Although the isotropic thermal parameters for several atoms in the isoprenoid tails were high (20 $Å^2$), these positions did not migrate significantly from a starting point during refinement.

25-Hydroxycholesterol. The numbering scheme for 25-hydroxycholesterol is shown in Fig. 1b. Its structure was solved by the DIRDIF (14) direct methods program. After identifying all positions in the electron density map, the non-hydrogen atoms were refined anisotropically. Theoretical hydrogen atoms were included but not refined. The final cycle of full matrix least squares refinement was based on 6566 observed reflections ($I > 3\sigma(I)$) and 540 variable parameters and converged to a weighted R factor of 0.034. The weighting scheme was based on counting statistics. Neutral atom scattering factors were taken from Cromer and Weber (15). Anomalous dispersion effects were included in F_{calc}. The values for $\Delta f'$ and $\Delta f''$ were those of Creagh and Mc

Auley (16). The values for the mass attenuation coefficients are those of Creagh and Hubbell (17). All calculations were performed using the teXsan (18) crystallographic software package of Molecular Structure Corporation.

RESULTS

7-Ketocholesterol

The molecular packing for 7-ketocholesterol in the unit cell is shown in **Fig. 2.** The final atomic positions and thermal parameters are listed in **Table 1,** and bond lengths and angles are depicted in **Fig. 3** and **Fig. 4,** respectively. It is clear that the ketone substitution of this cholesterol derivative induces a major change in the layer packing found for cholesterol monohydrate, i.e., a localized hydrogen bonding network between two hydroxyl group O3 atoms, a keto atom and the solvent atom (Fig. 2). The average oxygen to oxygen distance is 2.6 Å with the water molecule at the center of this network. The other keto oxygen is found in a hydrophobic pocket (Fig. 2) and is not involved in any polar interactions.

Because of the translational requirement induced by the localized hydrogen bonding scheme, the isoprenoid tails are twisted away from each other in a conformation that is not typical for cholesterol molecules (19–21). A comparison of conformational angles in this region to those for cholesterol monohydrate and anhydrous cholesterol, respectively, is found in **Table 2.**

25-Hydroxycholesterol

The molecular packing for 25-hydroxycholesterol in the unit cell is shown in **Fig. 5.** The final atomic positions and thermal parameters are listed in **Table 3,** and bond lengths and angles are depicted in **Fig. 6** and **Fig. 7** respectively.

The introduction of the oxygen at position 25 on the isoprenoid chain leads to a packing scheme for the 25-hydroxycholesterol molecules that differs from both cholesterol monohydrate as well as 7-ketocholesterol, i.e., a head to tail or approximately antiparallel fashion. (However, the molecular axes are not perfectly parallel.) This also results in the interdigitation of the steroid portions of the two molecules in the asymmetric unit.

Another result of the crystal packing of the 25-hydroxycholesterol molecules is that there are chains of hydrogen bonding that include the O3 and O25 oxygens of both molecule 1 and molecule 2 as well as the solvent oxygen (**Fig. 8**). The hydrogen bonding pattern can be traced starting with the O3 of molecule 1 pro-

TABLE 1. Fractional atomic positions and thermal parameters for 7-ketocholesterol

	X	Y	Z	B
Molecule 1				
C1A	0.3635	0.2542	0.4616	8.78
C2A	−0.4051	0.2305	−0.5048	6.06
C3A	−0.3390	0.0569	−0.5239	4.71
C4A	−0.2042	0.1144	−0.5215	5.37
C5A	−0.1659	0.1545	−0.4823	6.01
C6A	−0.0616	0.0763	−0.4687	3.41
C7A	−0.0041	0.1228	−0.4307	6.95
C8A	−0.0535	0.3081	−0.4090	5.39
C9A	−0.1930	0.2840	−0.4149	5.55
C10A	−0.2266	0.3129	−0.4587	5.28
C11A	−0.2508	0.4752	−0.3880	9.20
C12A	−0.2163	0.4254	−0.3470	7.45
C13A	−0.0788	0.4536	−0.3420	4.76
C14A	−0.0268	0.2740	−0.3633	6.88
C15A	0.1148	0.2816	−0.3523	9.15
C16A	0.0967	0.3267	−0.3069	8.56
C17A	−0.0251	0.3890	−0.2993	5.99
C18A	−0.0465	0.6814	−0.3516	8.82
C19A	−0.2147	0.5425	−0.4707	6.33
C20A	−0.0366	0.5658	−0.2713	9.69
C21A	−0.1612	0.6341	−0.2628	11.20
C22A	0.0190	0.4330	−0.2333	13.94
C23A	0.0329	0.5947	−0.2012	21.26
C24A	0.0729	0.4435	−0.1584	12.54
C25A	−0.0194	0.2972	−0.1506	20.36
C26A	0.0508	0.1951	−0.1192	20.85
C27A	−0.1014	0.4373	−0.1265	16.50
O3A	−0.3823	0.0359	−0.5616	6.86
O7A	0.0899	0.0378	−0.4211	8.29
Molecule 2				
C1B	0.4325	0.5898	0.3096	7.17
C2B	0.3999	0.6445	0.3440	5.53
C3B	0.4949	0.7900	−0.3559	7.16
C4B	0.5038	1.0087	−0.3356	5.64
C5B	0.5192	0.9537	−0.2919	4.14
C6B	0.6040	1.0589	−0.2703	6.18
C7B	0.6246	1.0292	−0.2296	8.04
C8B	0.5291	0.9080	−0.2112	6.95
C9B	0.4949	0.7141	−0.2344	6.65
C10B	0.4421	0.7940	−0.2787	3.19
C11B	0.3976	0.5779	−0.2136	7.33
C12B	0.4437	0.4941	−0.1738	6.28
C13B	0.4836	0.6942	−0.1524	5.72
C14B	0.5731	0.8148	−0.1681	6.59
C15B	0.6172	0.9926	−0.1389	7.50
C16B	0.6230	0.8560	−0.1016	10.28
C17B	0.5543	0.6599	−0.1120	5.44
C18B	0.3771	0.8489	−0.1447	7.14
C19B	0.3169	0.9106	−0.2705	9.13
C20B	0.4756	0.5747	−0.0777	11.28
C21B	0.4067	0.3790	−0.0840	10.18
C22B	0.5441	0.5829	−0.0365	8.47
C23B	0.6541	0.4107	−0.0424	10.21
C24B	0.7255	0.4147	−0.0010	9.29
C25B	0.8235	0.2462	0.0012	12.29
C26B	0.8362	0.0631	−0.0166	22.44
C27B	0.8668	0.2802	0.0475	15.96
O3B	0.4885	0.8552	−0.3978	7.13
O7B	0.7098	1.1132	−0.2117	14.07
Solvent water molecule				
OW1	0.3259	0.1452	0.5829	5.62

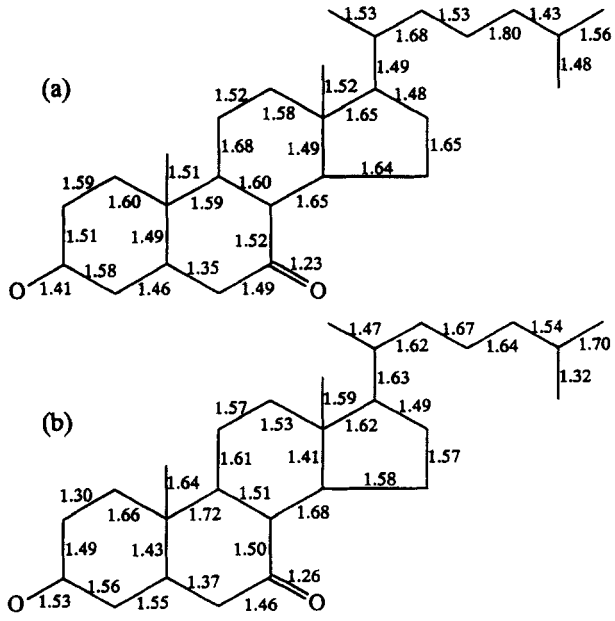

Fig. 3. Bond lengths for the two molecules in the unit cell for 7-ketocholesterol.

ceeding to the O3 of molecule 2 then to the solvent oxygen then to the O25 molecule 2 and to the O25 of molecule 1 and then back again to the O3 of molecule 1. The solvent molecule therefore facilitates the head to tail interactions of the two molecules. The average oxygen to oxygen distance is 2.5 Å. The solvent molecule packs in between the isoprenoid tails of molecule

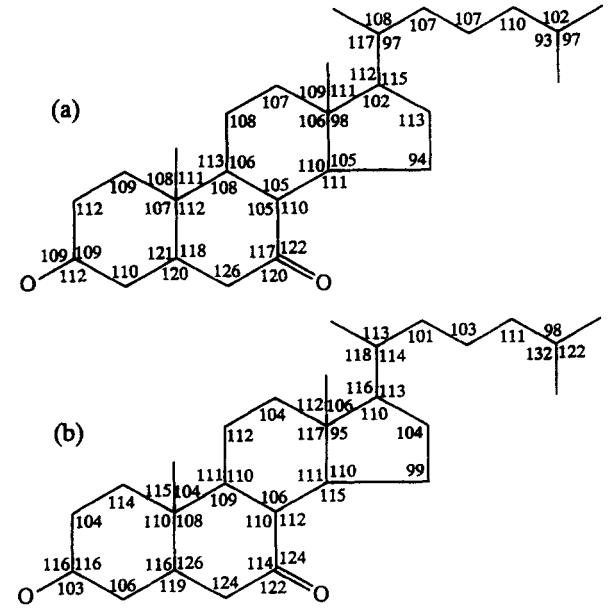

Fig. 4. Bond angles for the two molecules in the unit cell for 7-ketocholesterol.

TABLE 2. Torsion angles

	7-Keto	Cholesterol Monohydrate (11)	Cholesterol (Anhydrous) (12)
C13-C17-C20-C21	58.9	56.3	57.9
C17-C20-C22-C23	63.5/172.0	174.3	61.4/174.6
C20-C22-C23-C24	176.0	62.3/173.1	176.2
C22-C23-C24-C25	173.6/61.6	66.5/170.1	68.0/170.0

The torsion angles were averaged for all the molecules in the unit cell. In several cases, pairs of torsion angles were found.

2 (Fig. 8). The 25-hydroxy oxygens of molecule 2 align with the solvent oxygen which limits the conformational flexibility of that region.

DISCUSSION

Because of the very small difference in molecular volume, the cosolubility of 7-ketocholesterol in cholesterol is not difficult to understand. It is well known, for example, that a keto group can actually play a very small role in perturbing the structure of more regularly packed molecular crystals such as the n-paraffins as the ketoalkane crystal structures are very similar to those of their parents (22). In fact, ketoalkanes have been used for studies of crystal–crystal phase transitions in the n-paraffins as they are perfectly soluble probes (22). As illustrated by this crystal structure, however, keto substitution of a polar molecule can have a more pronounced effect on the molecular packing as the carbonyl oxygen can interact with either polar groups or nonpolar groups.

The effect of this substitution can be shown by com-

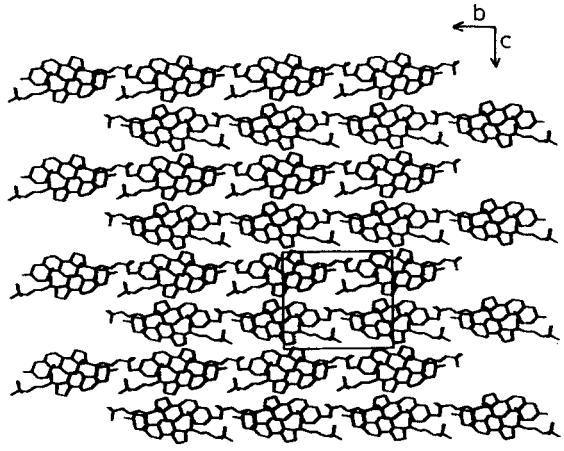

Fig. 5. Packing diagram of the 25-hydroxycholesterol molecules showing the anti-parallel packing of the molecules in the unit cell. The unit cell is enclosed in the box.

TABLE 3. Fractional atomic positions and thermal parameters for 25-hydroxycholesterol

	X	Y	Z	B_{eq}
Molecule 1				
O3A	−0.3583	−0.3154	−0.4758	2.36
O25A	0.4411	−0.2120	0.4578	2.34
C1A	−0.1155	−0.3379	−0.2934	1.95
C2A	−0.1765	−0.3484	−0.3828	2.19
C3A	−0.3020	−0.3002	−0.3919	2.00
C4A	−0.2827	−0.1984	−0.3730	2.05
C5A	−0.2173	−0.1830	−0.2863	1.80
C6A	−0.2618	−0.1225	−0.2351	1.94
C7A	−0.2026	−0.0980	−0.1500	2.01
C8A	−0.0720	−0.1382	−0.1303	1.72
C9A	−0.0687	−0.2362	−0.1665	1.78
C10A	−0.0981	−0.2371	−0.2631	1.76
C11A	0.0517	−0.2876	−0.1354	2.16
C12A	0.0859	−0.2828	−0.0404	2.02
C13A	0.0915	−0.1834	−0.0091	1.71
C14A	−0.0354	−0.1399	−0.0367	1.79
C15A	−0.0334	−0.0477	0.0099	2.09
C16A	0.0474	−0.0673	0.0934	2.29
C17A	0.0984	−0.1671	0.0871	1.87
C18A	0.1982	−0.1320	−0.0448	2.32
C19A	0.0065	−0.1922	−0.3078	2.20
C20A	0.2232	−0.1827	0.1412	2.07
C21A	0.2579	−0.2845	0.1447	3.07
C22A	0.2190	−0.1450	0.2297	2.29
C23A	0.3403	−0.1508	0.2858	2.17
C24A	0.3309	−0.0972	0.3671	2.20
C25A	0.4311	−0.1144	0.4389	2.18
C26A	0.5582	−0.0862	0.4165	2.64
C27A	0.3974	−0.0641	0.5171	2.76
Molecule 2				
O3B	0.7948	−0.2993	0.4050	3.75
O25B	0.2117	−0.2890	−0.5890	2.44
C1B	0.6957	−0.2421	0.1810	2.67
C2B	0.7717	−0.2377	0.2663	2.81
C3B	0.7199	−0.3049	0.3261	3.04
C4B	0.7221	−0.4016	0.2920	2.99
C5B	0.6533	−0.4087	0.2051	2.33
C6B	0.5685	−0.4736	0.1873	2.73
C7B	0.4983	−0.4885	0.1032	2.59
C8B	0.5517	−0.4349	0.0335	1.86
C9B	0.5899	−0.3379	0.0645	1.95
C10B	0.6894	−0.3394	0.1407	1.97
C11B	0.6262	−0.2766	−0.0007	2.29
C12B	0.5298	−0.2750	−0.0839	2.26
C13B	0.4997	−0.3718	−0.1167	1.76
C14B	0.4581	−0.4282	−0.0433	1.85
C15B	0.4068	−0.5172	−0.0836	2.26
C16B	0.3504	−0.4870	−0.1718	2.18
C17B	0.3842	−0.3837	−0.1816	1.85
C18B	0.6142	−0.4137	−0.1515	2.21
C19B	0.8191	−0.3648	0.1163	2.45
C20B	0.3924	−0.3539	−0.2722	2.05
C21B	0.4122	−0.2504	−0.2802	2.76
C22B	0.2790	−0.3850	−0.3308	2.13
C23B	0.2849	−0.3562	−0.4214	2.29
C24B	0.1925	−0.4070	−0.4833	2.55
C25B	0.2042	−0.3870	−0.5758	2.56
C26B	0.3228	−0.4259	−0.6041	3.05
C27B	0.0916	−0.4246	−0.6297	3.34
Solvent				
O (S)	1.0021	−0.2073	0.4535	4.04
C (S)	0.9830	−0.1131	0.4419	6.58

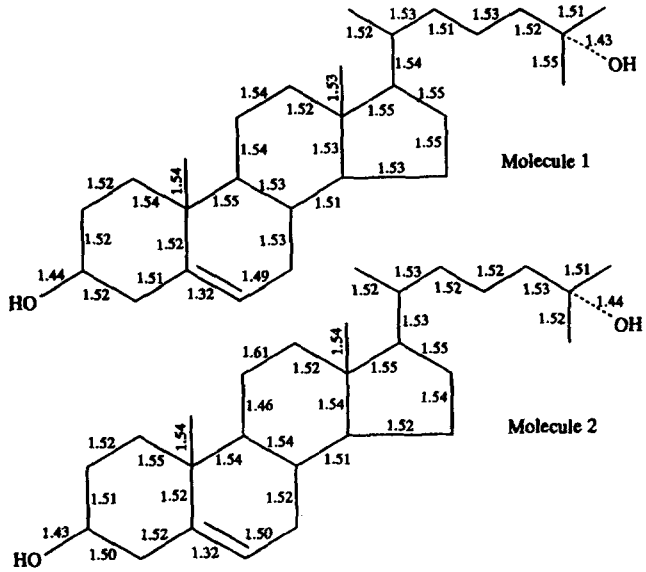

Fig. 6. Bond lengths for the two molecules in the unit cell for 25-hydroxycholesterol.

parison of this oxidized compound to the crystal structure of cholesterol monohydrate (20). Cholesterol packs in a bilayer structure in such a way as to maintain a continuous hydrogen bonding channel between the O3′ hydroxyl oxygens and the aqueous solvent. (Even though the layering of polar and nonpolar entities is not so well established for anhydrous cholesterol (20), continuous hydrogen bonding chains are also found for this non-solvated form.) The major effect of the keto group substitution, therefore, is to perturb this continu-

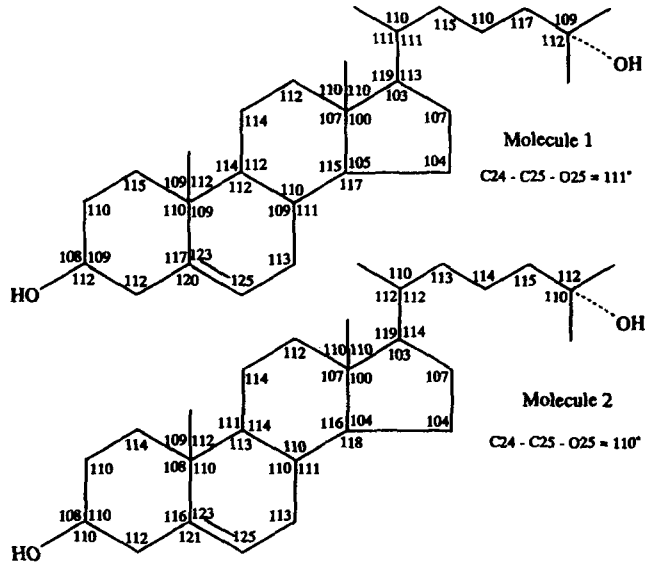

Fig. 7. Bond angles for the two molecules in the unit cell for 25-hydroxycholesterol.

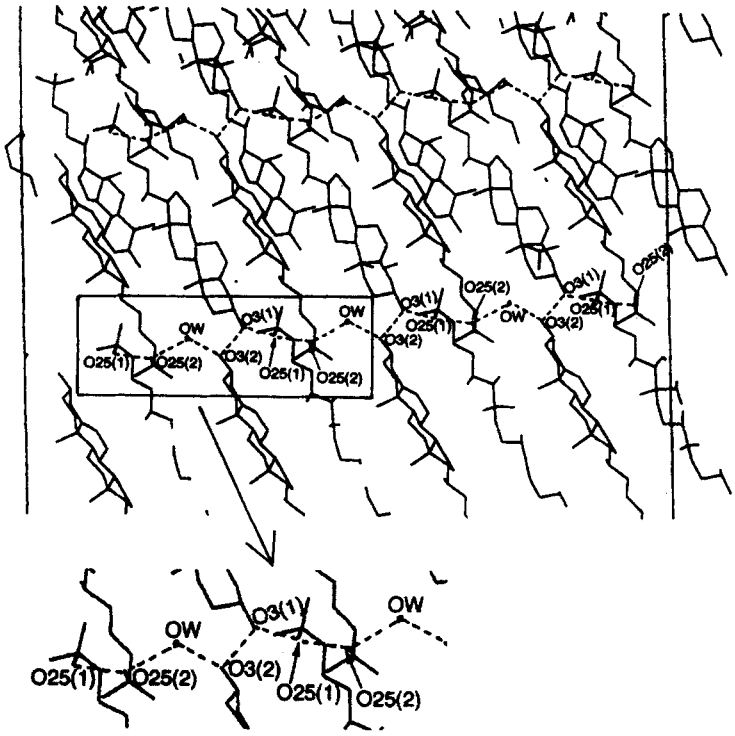

Fig. 8. Enlarged packing diagram for 25-hydroxycholesterol showing the continuous hydrogen bonding network that involves the 25-hydroxycholesterol molecules as well as the solvent molecule. The hydrogen bonding pattern follows the repeat from the O3 of molecule 1 to the O3 of molecule 2 then to the solvent oxygen then to O25 of molecule 2 to the O25 of molecule 1 and then back to the O3 of molecule 1. The figure shows two layers of repeat in this extended packing pattern which is tilted off of the bc plane.

ous hydrogen bonding network by constraining the directional interactions to localized hydrogen bonding regions, consisting of three cholesterol molecules and a solvent molecule, as seen in Fig. 2. The resultant molecular shifts needed to establish this localized interaction are also responsible for the unusual isoprenoid chain conformation at the interdigitating nonpolar interface (Table 2). Thus, while experimental phase diagrams demonstrate cosolubility of 7-ketocholesterol and cholesterol, it is clear from the crystal structure of the 7-ketocholesterol that the keto oxygen could disrupt cholesterol packing if the oxidized derivative were embedded as an adduct, eventually leading to fractionation.

The cosolubility of 25-hydroxycholesterol with cholesterol also is not difficult to understand, again given the small difference in molecular volumes. The effect of the hydroxyl substitution at position 25 on the structure of 25-hydroxycholesterol can also be shown by a comparison of this oxidized compound to the crystal structure of cholesterol monohydrate. As previously stated, cholesterol packs in a bilayer structure in such a way as to maintain a continuous hydrogen bonding channel between two O3′ hydroxyl oxygens and the aqueous solvent. The major effect of the 25-hydroxyl group is to perturb the hydrogen bonding so that even though a continuous chain of hydrogen bonding is maintained, the nature of the interactions are quite different especially since there is head to tail packing of the molecules in the 25-hydroxycholesterol structure that is not seen in the packing for the pure cholesterol. The packing for the 25-hydroxycholesterol structure also contrasts starkly with the molecular packing seen for the 7-ketocholesterol.

These two oxysterol crystal structures, therefore, indicate that a basis for the differences in their cytotoxicity may be found as a function of several structural factors including the ability to perturb the normal interactions for pure cholesterol. In future work we will determine the crystal structures of other cytotoxic oxidized cholesterols and then study their binary solids with cholesterol as a possible structural basis for further differentiating the toxicities of oxidized cholesterols.

Research reported in this paper was supported in part by a grant from the National Institutes of General Medical Sciences (GM48733) which is gratefully acknowledged.

Manuscript received 1 October 1996 and in revised form 15 January 1997.

REFERENCES

1. Steinberg, D., S. Parthasarathy, T. E. Carew, J. C. Khoo, and J. L. Witztum. 1989. Beyond cholesterol: modification of low density lipoprotein that mimics its other geometry. *N. Engl. J. Med.* **320:** 915–924.
2. Taylor, C. B., S. K. Peng, N. T. Werthessen, P. Tham, and K. T. Lee. 1979. Spontaneously occurring angiotoxic derivatives of cholesterol. *Am. J. Clin. Nutr.* **32:** 40–57.

3. Shih, J. C. H. 1980. Increased atherogenicity of oxidized cholesterol. *Fed. Proc.* **39:** 650–652.
4. Peng, S. K., C. B. Taylor, J. C. Hill, and R. J. Morin. 1985. Cholesterol oxidation derivatives and arterial endothelial damage. *Atherosclerosis.* **54:** 121–124.
5. Zwijsen, R. M. L., I. M. J. Oudenhoven, and L. H. J. de Haan. 1992. Effects of cholesterol and oxysterols on gap junctional communication between human smooth muscle cells. *Eur. J. Pharmacol.* **228:** 115–120.
6. Sparrow, C. P., S. Parthasarathy, and D. Steinberg. 1988. Enzymatic modification of low density lipoprotein by purified lipoxygenase phospholipase A_2 mimics cell-mediated oxidative modification. *J. Lipid Res.* **29:** 745–753.
7. Quinn, M. T., S. Parthasarathy, L. G. Fong, and D. Steinberg. 1989. Oxidatively modified low density lipoproteins: a potential role in recruitment and retention of monocyte/macrophages during atherogenesis. *Proc. Natl. Acad. Sci. USA.* **84:** 2995–2998.
8. Peng, S. K., R. J. Morin, P. Tham, and C. B. Taylor. 1985. Effects of oxygenated derivatives of cholesterol on cholesterol uptake by cultured aortic smooth muscle cells. *Artery.* **13:** 144–164.
9. Peng, S. K., and R. J. Morin. 1987. Effects on membrane function by cholesterol oxidation derivatives in cultured aortic smooth muscle cells. *Artery.* **14:** 85–89.
10. Dorset, D. L. 1992. Binary phase behavior of angiotoxic oxidized cholesterols with cholesterol. *Biochim. Biophys. Acta.* **1127:** 293–297.
11. Blessing, R. 1989. DREADD-data reduction and error analysis for single-crystal diffractometer data. *J. Appl. Crystallogr.* **22:** 396–397.
12. Miller, R., G. T. Detitta, R. Jones, D. A. Langs, C. M. Weeks, and H. A. Hauptman. 1993. On the application of the minimal principle to solve unknown structures. *Science.* **259:** 1430–1433.
13. Weeks, C. M., G. T. Detitta, R. Miller, and H. A. Hauptman. 1993. Applications of the minimal principle to peptide structures. *Acta Crystallogr.* **D49:** 179–181.
14. Beurskens, P. T., G. Admiraal, G. Beurskens, W. P. Bosman, S. Garcia-Grande, R. O. Gould, J. M. M. Smits, and C. Smykalla. 1992. The DIRDIF program system, Technical report of the Crystallography Laboratory, University of Nijmegan, The Netherlands.
15. Cromer, D. T., and J. T. Weber. 1974. Mean atomic scattering factors in electrons for free atoms and chemically significant ions. International Tables for X-ray Crystallography. Vol. IV. Kynoch Press, Birmingham, England. Table 2.2A, 72–98.
16. Creagh, D. C., and W. J. McAuley. 1992. Dispersion corrections for forward scattering, International Tables for Crystallography. Vol. C. Kluwer Academic Publishers, Norwell, MA. Table 4.2.6.8, 219–222.
17. Creagh, D. C., and J. H. Hubbell. 1992. Mass attenuation coefficients (cm^2/gm), International Tables for Crystallography. Vol. C. Kluwer Academic Publishers, Norwell. MA. Table 4.2.4.3, 200–206.
18. teXsan: Crystal Structure Analysis Package. Molecular Structures Corporation (1985 and 1992) The Woodlands, Texas.
19. Craven, B. M. 1979. Pseudosymmetry in cholesterol monohydrate. *Acta Crystallogr.* **B35:** 1123–1126.
20. Shieh, H. S., L. G. Hoard, and C. E. Nordman. 1981. The structure of cholesterol. *Acta Crystallogr.* **B37:** 1538–1541.
21. Duax, W., Z. Wawrzak, J. F. Griffen, and C. Cheer. 1988. Sterol conformation and molecular properties. *In* Biology of Cholesterol. Philip L. Yeagle, editors. GRC Press Co. Inc., Boca Raton, Fl. 1–18.
22. Malta, V., G. Cojazzi, R. Zannetti, and L. Amati. 1974. Molecular packing in long chain compounds: the crystal structure of symmetrical 12-tricosanone. *Gazz. Chim. Ital.* **104:** 921–924.
23. Strobl, G., T. Trzebiatowski, and B. Ewen. 1978. Analyse der Temperaturabhängigkeit der dielektrischen α-Relaxation am Modell eines Paraffin-Keton-Mischkristalls. *Prog. Colloid Polymer Sci.* **64:** 219–225.